AIAA JOURNAL
Vol. 31, No. 2, February 1993

Structured Background Grids for Generation of Unstructured Grids by Advancing-Front Method

Shahyar Pirzadeh*
ViGYAN, Inc., Hampton, Virginia 23666

A new method of background grid construction is introduced for generation of unstructured grids using the advancing-front technique. Unlike the conventional triangular/tetrahedral background grids that are difficult to construct and usually inadequate in performance, the new method exploits the simplicity of uniform Cartesian meshes and the superiority of the elliptic grid point distribution for unstructured grid generation. The approach is analogous to solving a steady-state heat conduction problem with discrete heat sources. The spacing parameters of grid points are distributed over the nodes of a Cartesian background grid by solving a Poisson equation. To increase the control over the grid point distribution, a directional clustering approach is developed. The new method is convenient to use and provides better grid quality and flexibility. Some sample two-dimensional results are presented to demonstrate the power of the method.

Introduction

AN important feature of any grid-generation technique is its ability to distribute grid points smoothly throughout a computational domain. The need for smoothness is dictated by requirements for numerical stability and accuracy of flow solutions and is independent of the mesh type, e.g., structured or unstructured. For structured mesh generation, the question of grid point distribution is usually addressed by the solution of appropriate equations (algebraic, differential, etc.), which generally results in smoothly varying meshes. Many unstructured grid-generation techniques, however, do not rely on any rigorous mathematical approach for distributing grid points and thus may lack the desired smoothness.

One of the techniques for generating unstructured triangular/tetrahedral grids is the advancing-front method.[1-5] In this approach a grid is generated by forming cells starting from the domain boundaries and marching toward the interior of the computational domain. The local grid characteristics, such as grid point distribution, are controlled by information stored at the nodes of a secondary coarse mesh referred to as the "background" grid. Typically, a background grid consists of unstructured triangular or tetrahedral cells that enclose the entire domain without the requirement of conforming to the configuration. Its sole function is to guide a marching front for insertion of new points at proper locations. As the front advances into the field, the grid parameters defining the position of a new point are interpolated from the values stored at the nodes of the background grid cell that encloses the point.

The quality of a generated grid and the convenience by which it is obtained largely depend on the adequacy of the background grid used. The smoothness in variation of grid-spacing parameters from point to point in the field not only determines the quality of the final mesh but also affects the robustness of the grid-generation process itself. An unsatisfactory distribution of grid parameters at the nodes of a background grid (for example, a sudden change in spacing) often creates physically impossible conditions that result in frequent failures of a grid-generation process. Therefore, as an essential part of the advancing-front method, background grids introduce some additional important grid-generation issues that should be considered. Among these are the questions of simplicity, accuracy, efficiency, and flexibility of background grids. For convenient generation of a good quality mesh, 1) the background grid should be easy to construct with a reasonable amount of the user's time and effort, 2) the background grid should provide a smooth and controllable distribution of grid points throughout the domain, 3) the interpolation from a background grid to a point in the domain should be done efficiently, and 4) the modification of a background grid should be convenient after it is constructed for a problem. These issues have a considerable impact on the robustness and usability of an unstructured grid generator requiring a background grid.

This paper presents a new type of background mesh that resolves many of the problems associated with the conventional approach. The new method is based on uniform Cartesian meshes and automatically distributes grid parameters in the field by solution to an elliptic partial differential equation. A directional distribution approach is used to enhance the control over grid point clustering. Only two-dimensional problems are considered in this paper. The extension of the method to three-dimensional problems is relatively straightforward. The following sections describe the new methodology in detail. A brief explanation of the shortcomings of the conventional background grid is presented first to demonstrate the impetus for the present work.

Unstructured Background Grids

A background grid made of a number of triangular cells that covers the domain around a two-dimensional configuration is shown in Fig. 1. A background grid of this type is usually generated either manually or graphically. Several methods for generating such grids are given in Ref. 3.

For small problems involving generation of grids around simple geometries, a background grid composed of a few triangular or tetrahedral cells may easily be constructed by hand with controllable distribution of spacing parameters among the background grid nodes. However, as the complexity of the geometry increases or for meshes that are adapted to a flow solution, larger and more sophisticated background grids are required.[2] Obviously, the manual construction of a background grid having a few hundred nodes is both difficult and time consuming.

Furthermore, the task of individually prescribing spacing parameters for a large number of background nodes is both tedious and inaccurate. It is not uncommon to prescribe an unsatisfactory distribution of spacing parameters that results

Presented as Paper 91-3233 at the AIAA 9th Applied Aerodynamics Conference, Baltimore, MD, Sept. 23-25, 1991; received Oct. 14, 1991; revision received Aug. 6, 1992; accepted for publication Aug. 11, 1992.

*Research Engineer, 30 Research Drive. Member AIAA.

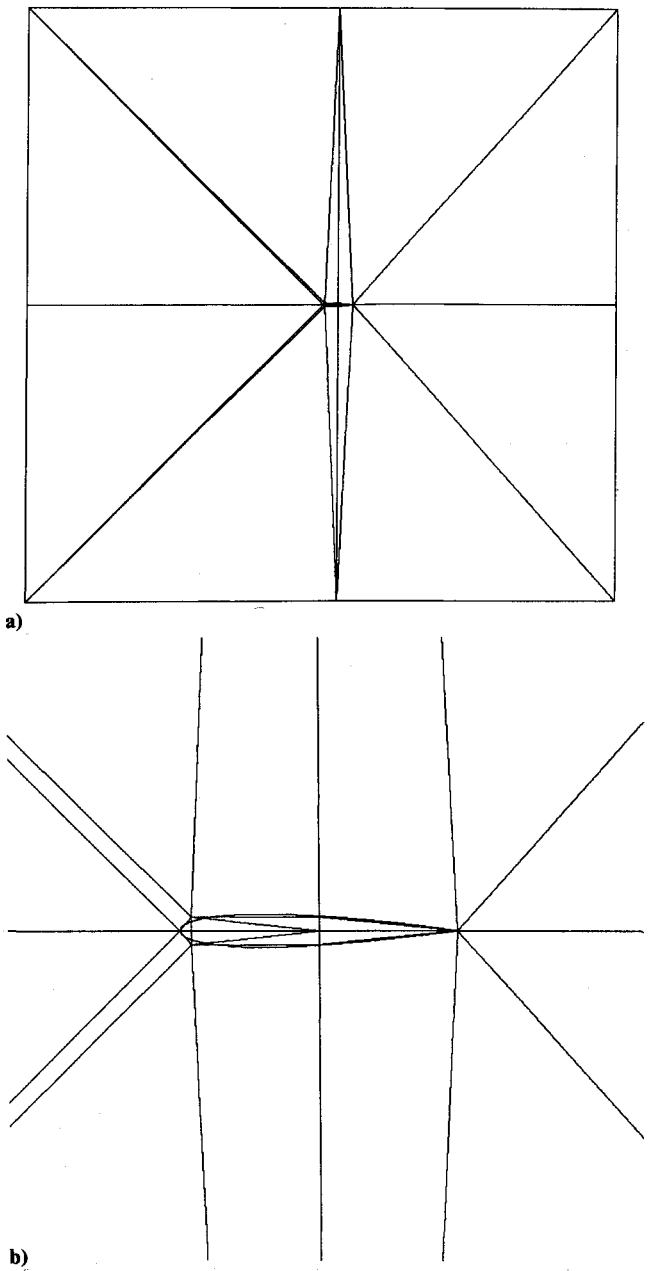

Fig. 1 Typical triangular background grid: a) far field, b) near field.

in a poor quality grid and in some cases severely affects the process of front advancement. Often, several attempts are required to produce an acceptable distribution. The two processes of constructing a good background grid and smoothly distributing spacing parameters by the conventional method account for a large portion of the total grid-generation time and require a great deal of the user's experience. In addition, the control over point distribution in the computational mesh using an unstructured background grid is difficult unless a large number of background grid points are introduced.

The third problem associated with a conventional background grid is its lack of flexibility for change and modification after it is constructed. Should a portion of a background grid be altered or if more nodes are subsequently desired in a section of the domain (for example, for addition of a nacelle/engine to a wing), a new background grid must be generated for the entire configuration to supply additional information.

Finally, interpolation from the nodes of an unstructured background grid requires storage of the mesh coordinates and connectivities. For each new grid point being introduced during the process of grid generation, a series of search and check operations must be performed to find the background grid cell that encloses the point. Each operation requires computation of several Jacobians of the background grid cells and shape functions.

Structured Background Grids

Since a background grid is used only for interpolation of grid characteristics and need not conform to the boundaries of the configuration, a simple uniform Cartesian grid can also accomplish the objective sufficiently. A Cartesian mesh is easily generated with a few simple lines of computer coding as opposed to the time-consuming manual construction of triangular/tetrahedral unstructured meshes. Associated with a Cartesian background grid is an arbitrary number of user-prescribed source elements at which grid parameters are defined. The source elements propagate spacing parameters in the field automatically and in a systematic manner. Two types of sources are used in this work: nodal and linear elements. The sources may be positioned anywhere in the field, preferably near the surfaces of the geometry and at the outer boundaries. Generally speaking, the location of a source element is chosen where a well-controlled distribution of grid points is desired

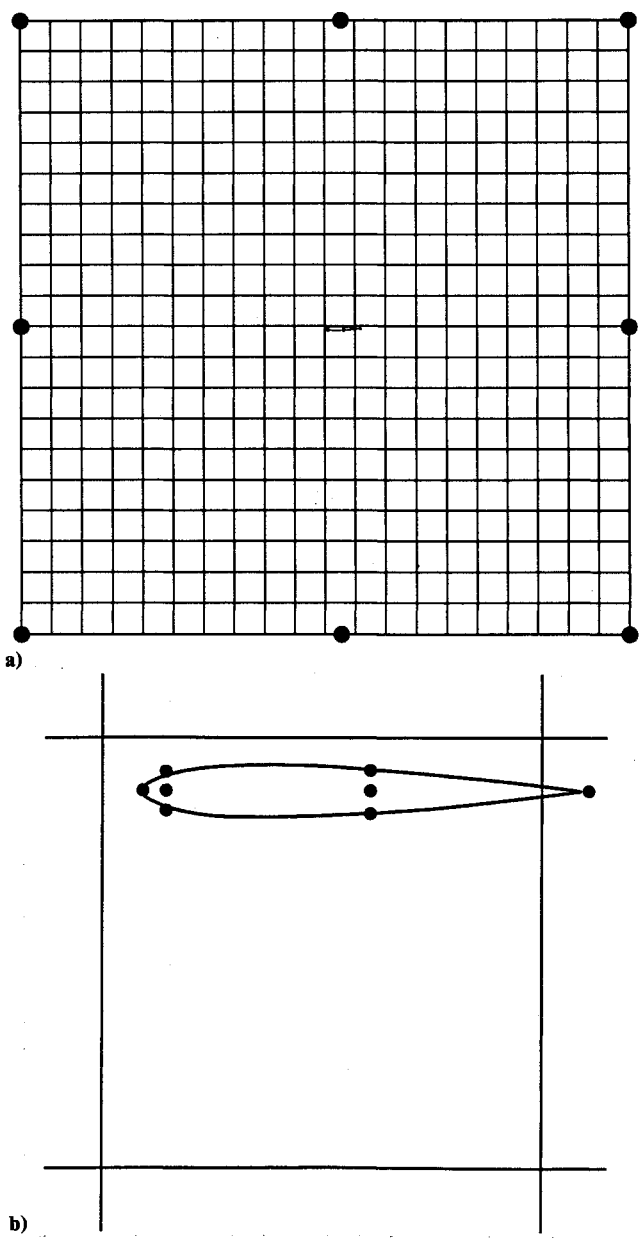

Fig. 2 Typical Cartesian background grid with source elements: a) far field, b) near field.

such as the leading edge of an airfoil/wing or at an expected shock wave location.

Figure 2 shows a structured background grid covering the computational domain around the same configuration as the one in Fig. 1. Note that the positions of the background grid points match neither the boundaries of the geometry to be gridded nor the source elements. The number and locations of the sources, in this example, are chosen the same as those of the unstructured background grid nodes in Fig. 1 for comparison of the generated grids. Fewer source elements are typically required for such a simple geometry.

Distribution of Grid Parameters

The spatial variation of grid parameters in a field is determined by a process similar to that of computing the diffusion of heat from discrete heat sources in a conducting medium. The process is modeled by solving a Poisson equation on the Cartesian grid with specified sources and Dirichlet boundary conditions. The solution to such a problem provides "pseudo-isotherms" that vary smoothly from high- to low-potential regions. The procedure is similar to that of elliptic structured grid-generation schemes in which a system of elliptic partial differential equations are solved on a uniformly spaced grid in the computational domain to obtain the coordinates of the grid points in the physical space. For the present method, a single elliptic equation is solved for grid point spacing parameters in the physical domain with no transformation between different frames of reference. The concentration of grid points in a region can easily be controlled by strength and intensity of local sources.

A smooth distribution of grid-spacing parameters within a domain is modeled by

$$\nabla^2 S = G \tag{1}$$

along with a set of given boundary conditions

$$S = S_b \tag{2}$$

where S denotes the grid-spacing parameter, G is a source term maintaining the spacings in the field, and S_b represents prescribed spacing values at the outer boundaries. A discretization of Eq. (1) is obtained by assuming that propagation of spacing parameters to a background grid node from the source elements and the adjacent grid nodes (Fig. 3) is determined by a weighted averaging procedure based on the inverse of distance squared. The outcome is a five-point approximation of Eq. (1) on the Cartesian background grid with the resulting source term

$$G_{i,j} = \sum_{n=1}^{N} \psi_n (S_{i,j} J_n - I_n) \tag{3}$$

where (i,j) represents a background grid node index, N is the total number of source elements in the field, and ψ_n is an intensity factor for the nth source element. The functions I_n and J_n in Eq. (3) are defined as

$$I_n = \begin{cases} S_n / r_n^2 & \text{nodal source} \\ \dfrac{1}{|\ell_n|} \displaystyle\int_{\ell_n} \frac{f(\ell)}{r(\ell)^2}\, d\ell & \text{linear source} \end{cases} \tag{4}$$

and

$$J_n = \begin{cases} 1/r_n^2 & \text{nodal source} \\ \dfrac{1}{|\ell_n|} \displaystyle\int_{\ell_n} \frac{d\ell}{r(\ell)^2} & \text{linear source} \end{cases} \tag{5}$$

where S_n is the prescribed spacing at the nodal source n with a distance r from the interpolation point and $f(\ell)$ denotes a linear variation of spacing along the line source n with a length $|\ell_n|$. The line integrals in Eqs. (4) and (5) are evaluated analytically for straight line elements for which spacing parameters are prescribed at the endpoints.

The implementation of the Gauss-Seidel iterative scheme with successive over-relaxation to the problem yields

$$S_{i,j}^{m+1} = (1-\omega) S_{i,j}^{m} + \omega \Big(S_{i-1,j}^{m+1} + S_{i+1,j}^{m} + S_{i,j-1}^{m+1} + S_{i,j+1}^{m} + h^2 \sum_{n=1}^{N} \psi_n I_n \Big) \Big/ \Big(4 + h^2 \sum_{n=1}^{N} \psi_n J_n \Big) \tag{6}$$

where h is the uniform background grid spacing, m is an iteration level, and ω is a relaxation parameter $(0<\omega<2)$. The iterative solution is stable due to the diagonal dominance of the resulting coefficient matrix. An optimum value for ω which significantly accelerates the convergence rate of the iterative process can, in general, be obtained by some numerical examination. For a two-dimensional problem on a rectangular domain, however, a theoretical analysis is available for evaluation of an optimum ω.[6]

The spacing parameters at the nodes of a background grid are first interpolated from all source elements using

$$S_{ij} = \sum_{n=1}^{N} (\psi_n I_n) \Big/ \sum_{n=1}^{N} (\psi_n J_n) \tag{7}$$

This rather crude distribution serves as initial values for the iterative scheme. Equation (6) is then solved iteratively on the interior background grid points, subject to the fixed boundary values determined by Eq. (7), until convergence when a final smooth distribution of grid spacings is obtained.

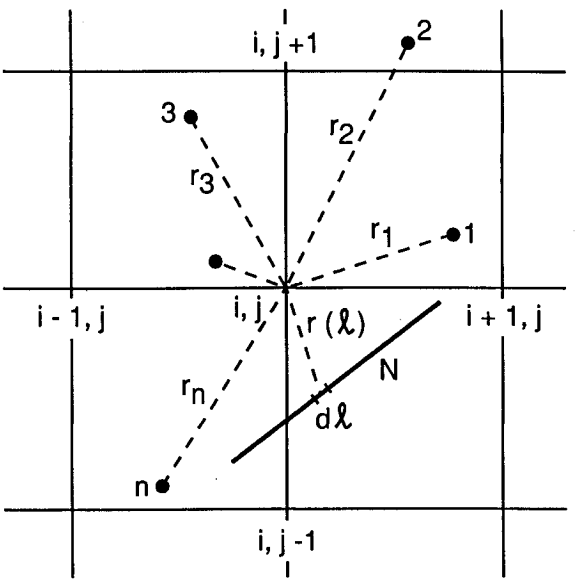

Fig. 3 Source elements in a Cartesian background grid.

Distribution Control

The spacing parameter prescribed for a source at a location represents the local dimensional grid size with its effect gradually diffused as the distance from the source is increased. The control over distribution of points in a grid is achieved by adjusting the locations, spacing parameters, and intensities specified for the source elements. The intensity of a source ψ_n controls the extent by which the effect of the element propagates in a field. It can be viewed as a factor influencing the effective distance between a source element and a point in the field as indicated in Eq. (7). Unlike the spacing parameter of a source element that is absolute, the intensity is a nondimen-

sional factor, and its function is relative to those of other sources in the field. The higher the relative intensity for a source, the farther the influence of the source can extend into the domain. Figures 4a and 4b compare two grids generated in a square domain with side lengths of unity by specifying one nodal source element in the middle and four at the corners of the field. The source elements in both cases have identical spacing parameters: 0.2 at the corners and 0.005 in the middle. The source elements at the corners have intensity of 1.0 in both cases. The intensity of the source in the middle is prescribed as 8.0 for case a and 2.0 for case b, resulting in completely different grid distributions.

In addition to a simple symmetrical intensity adjustment, a directional control capability is developed that considerably enhances the overall flexibility of point distribution in a grid. This is done by limiting the source intensities to certain zones and directions as follows. Consider a nodal source n located at a distance r_n from an interpolation point p as depicted in Fig. 5, which also shows a unit vector u defining the desired propagation direction. A directional (zonal) intensity for the

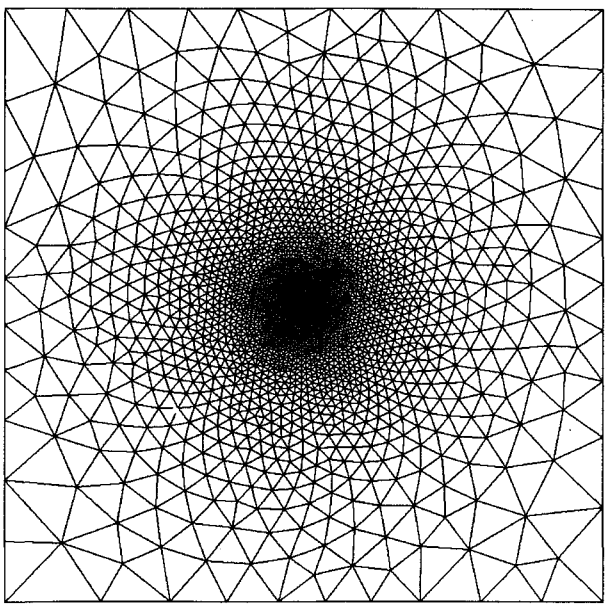

a)

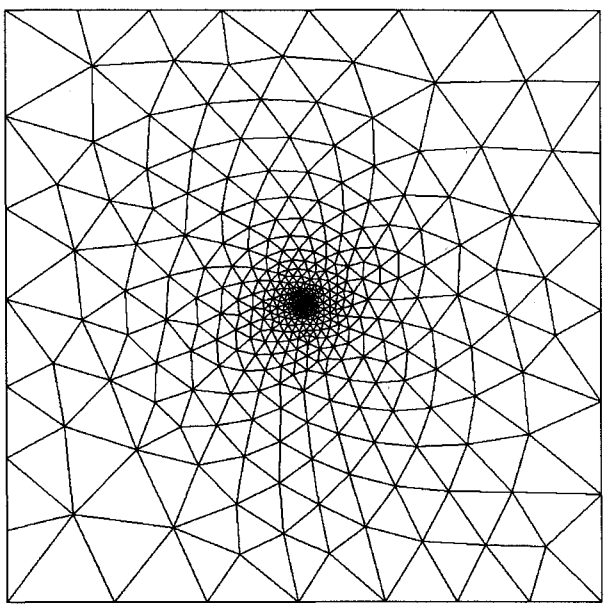

b)

Fig. 4 Effect of source intensity on grid distribution: a) high intensity, b) low intensity.

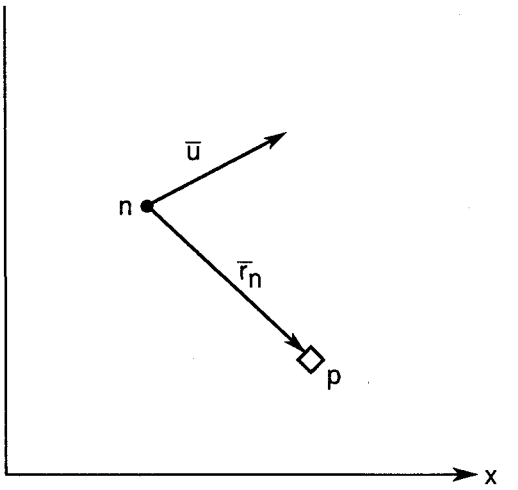

Fig. 5 Interpolation point p in relation to a nodal source n propagating in direction of vector u.

source element n in relation to the interpolation point p is calculated as

$$\psi_n = a_n\beta + b_n|\phi|^k \tag{8}$$

where a_n and b_n are prescribed parameters specifying the magnitude of the domain of influence of the source element, k is a positive constant (a value of 10 is used in this work), and β and ϕ limit the source propagation in accordance with the prescribed zone and direction. The parameter ϕ is defined by

$$\phi = \left(1 - \frac{|\alpha|}{2}\right) v \cdot u + \frac{\alpha}{2}|v \cdot u| \tag{9}$$

where

$$v = r_n / r_n \tag{10}$$

and β is equal to 1 unless b_n is zero for which

$$\beta = \begin{cases} 0 & \text{if } \alpha(v \cdot u) < 0 \\ 1 & \text{if } \alpha(v \cdot u) \geq 0 \end{cases} \tag{11}$$

A value of 1 for α indicates propagation on one side of the source in the direction of the prescribed unit vector u whereas -1 specifies propagation on the opposite side. For α equal to 0, propagation would be on both sides of the source. The first term on the right-hand side of Eq. (8) gives a circular or semicircular (one-sided) propagation around a nodal source with a_n controlling the propagation radius, whereas the second term provides an extended, one- or two-sided propagation along the prescribed direction with b_n influencing the extent of the propagation. For a linear source, a_n and b_n also independently contribute to the propagation on either or both sides of the element. The magnitude of the intensity parameters a_n and b_n are determined best by experiment for individual problems. In practice, a balance between the total intensity of the inner source elements (around the geometry) and that of the sources positioned at the outer boundaries would result in a satisfactory grid distribution in the field for two-dimensional problems.

Figures 6a–6c depict three sample grids generated with various directional intensities prescribed for a nodal source element located at the center of a unit square with a propagation direction specified toward the upper left corner. The intensities of the four outer sources and the spacing parameters in these grids are identical to those in Fig. 4. The parameters for the middle source are given in Table 1. Note that, in addition to the side, direction, and extent, the expanse width of the nodal

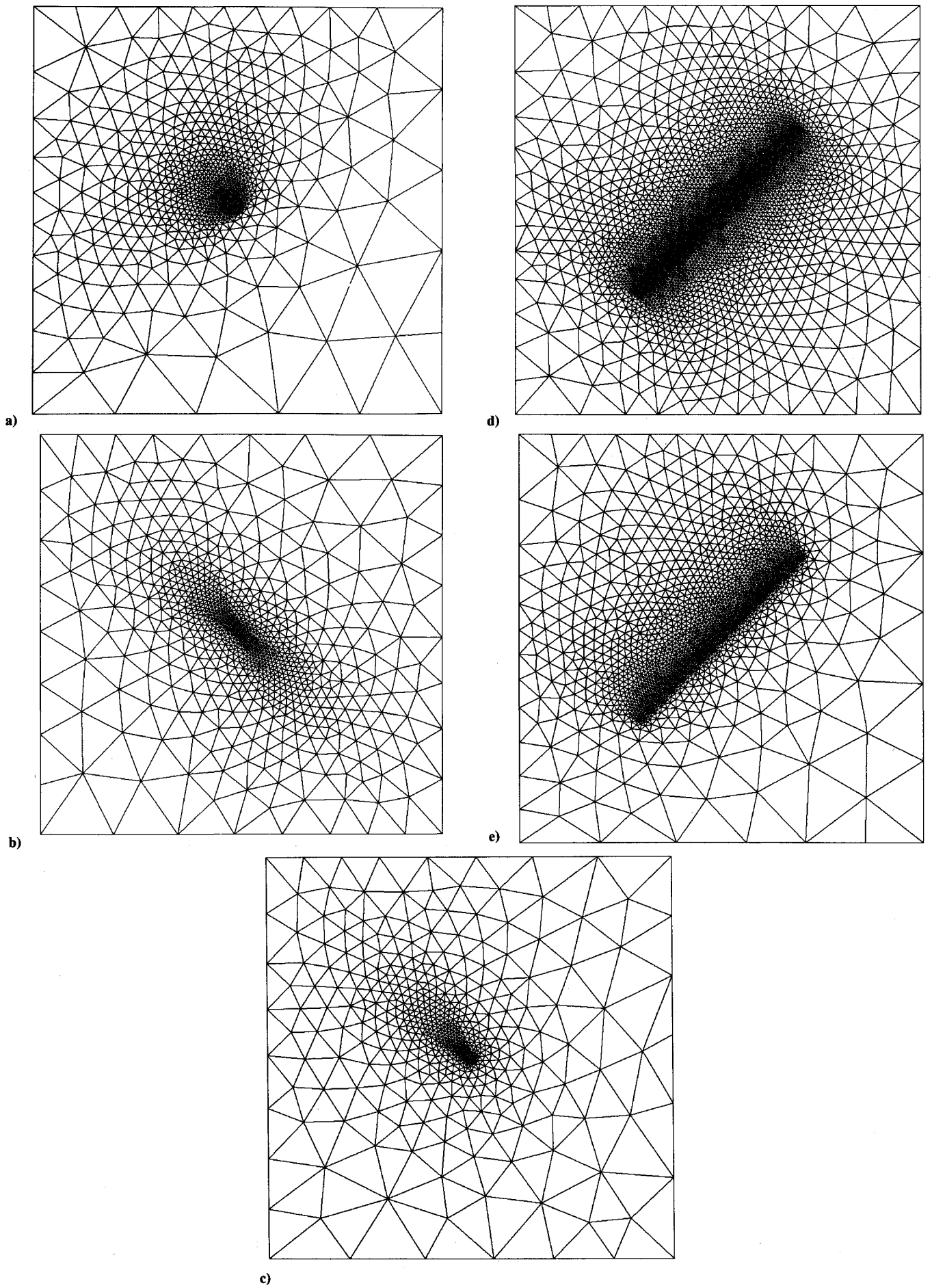

Fig. 6 Effect of directional intensity on grid distribution.

Table 1 Middle source parameters for the grids in Fig. 6

Grid	a_n	b_n	α
a	8.0	0.0	1.0
b	1.0	16.0	0.0
c	1.0	16.0	1.0
d	0.2	4.0	0.0
e	0.2	4.0	1.0

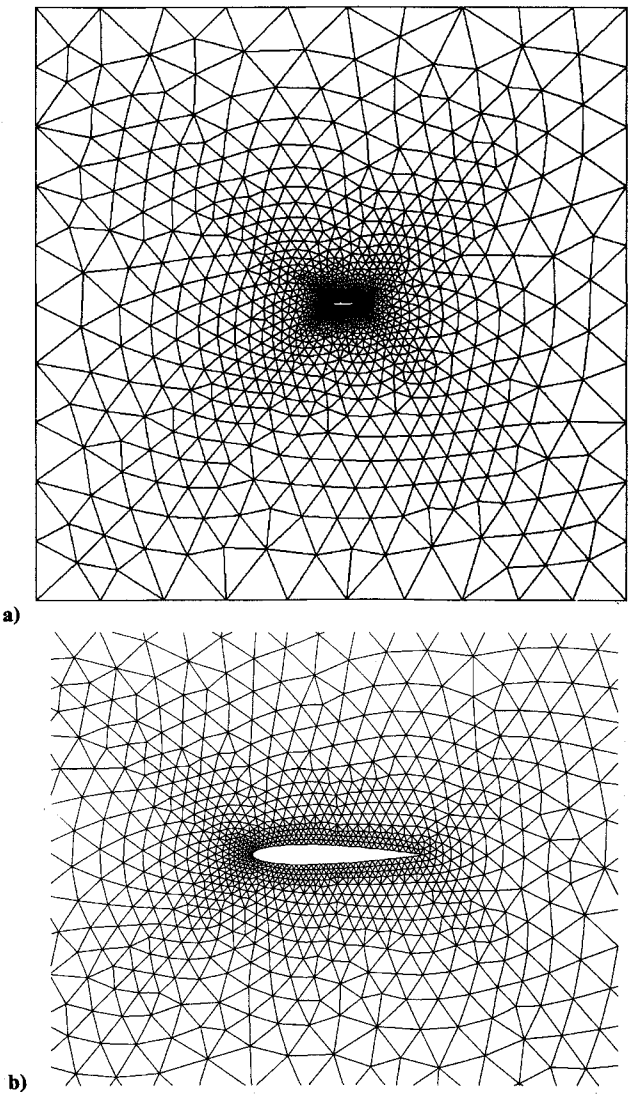

Fig. 7 Triangular grid around NACA 0012 airfoil generated using a conventional unstructured background grid: a) far field, b) near field.

source is also controlled as shown in Figs. 6a and 6c. A similar approach applies to linear sources with control over the propagation of grid spacings on either side of the element. Figures 6d and 6e show a linear source element with two- and one-sided propagations, respectively, producing different grid distributions.

Interpolation

During the process of advancing front, the size of a grid element (side or cell) at an arbitrary location in the field is interpolated from the spacing parameters stored in the background grid. Unlike the unstructured background grids for which the storage of coordinates/connectivities and performance of a series of search and check operations are required to locate an interpolation point in an enclosing cell, uniform Cartesian background grids provide a simple search/interpolation procedure. An interpolation point p is located in a Cartesian cell with a primary node index given by integers

$$i = (x_p - x_{\min})/h + 1 \tag{12a}$$

$$j = (y_p - y_{\min})/h + 1 \tag{12b}$$

where x_p and y_p are the coordinates of point p, and $x_{\min}$ and $y_{\min}$ are the minimum coordinates of the background grid. The remaining nodes of the cell covering point p are represented by indices with one level higher than the primary index. Interpolation from the four nodes is performed by any conventional method such as bilinear, inverse distance weighting, etc.

Since a background grid is usually very coarse in relation to the geometry of interest, interpolation from only four nodes of a background grid cell may not provide sufficient control of grid point clustering within the cell. This is especially the case in regions close to the geometry or at an expected shock wave where a more flexible point distribution and a rapid change in grid spacings are required. For a better point distribution using a coarse background grid, the spacing parameter at a location may be interpolated from the four nodes of the background grid cell that encloses the interpolation point on the front while also taking contributions from the source elements using a weighted averaging procedure similar to that given by Eq. (7). Contributions from all source elements and from those falling in the enclosing background grid cell have both resulted in good grid point distributions.

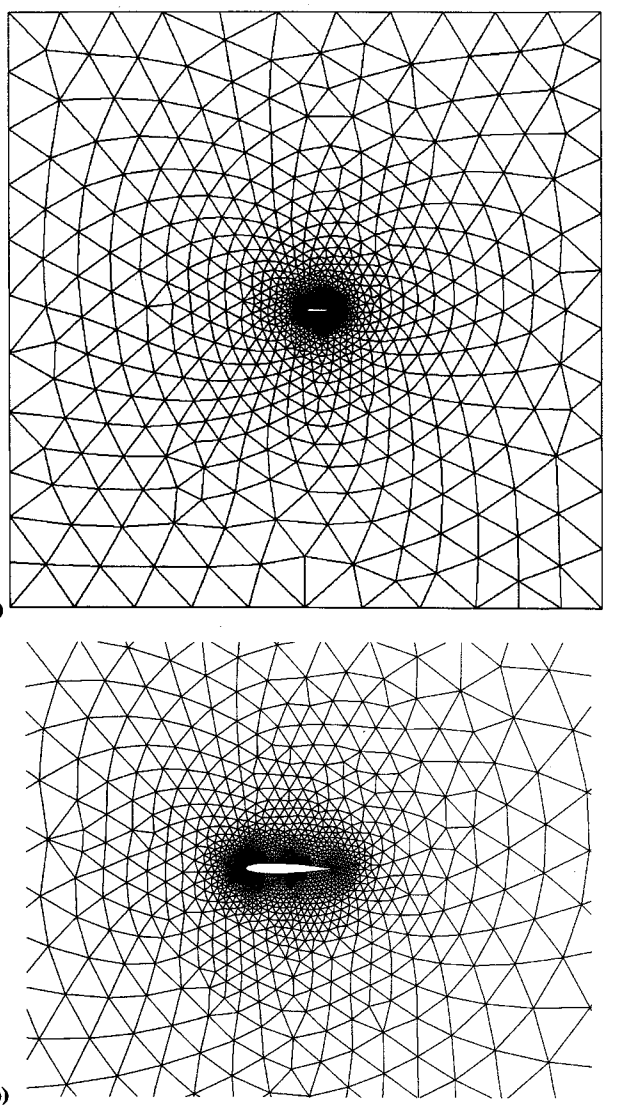

Fig. 8 Triangular grid around NACA 0012 airfoil generated using a structured background grid: a) far field, b) near field.

Interpolation of spacing parameters from the background grid nodes and the source elements brings up the question of requirements on the resolution of background grids or even whether the advancing-front process can be conducted without a background grid by a simple data transfer directly from sources. The problem is analogous to comparing algebraic structured grid-generation methods with those having elliptic smoothing capabilities. A simple interpolation directly from source elements in the absence of an "elliptic" background grid may lack the desired smoothness of the final grid as demonstrated in the next section. The density (resolution) of a background grid depends on the size of the configuration to be gridded, the desired smoothness of the final grid, and whether interpolation is from both background grid nodes and source elements. For a large domain containing a small configuration and no direct interpolation from sources, a finer background grid is required to produce a smooth grid with adequate grid-spacing variation in the field.

Results

Several two-dimensional grids have been generated around two configurations and are presented in this section to show the capability of the new method. The objective is to demonstrate the quality and versatility of grids generated for problems featuring complicated flowfields and complex geometries. All of the meshes in this study were generated with a modified two-dimensional version of the advancing-front method reported in Refs. 1 and 3.

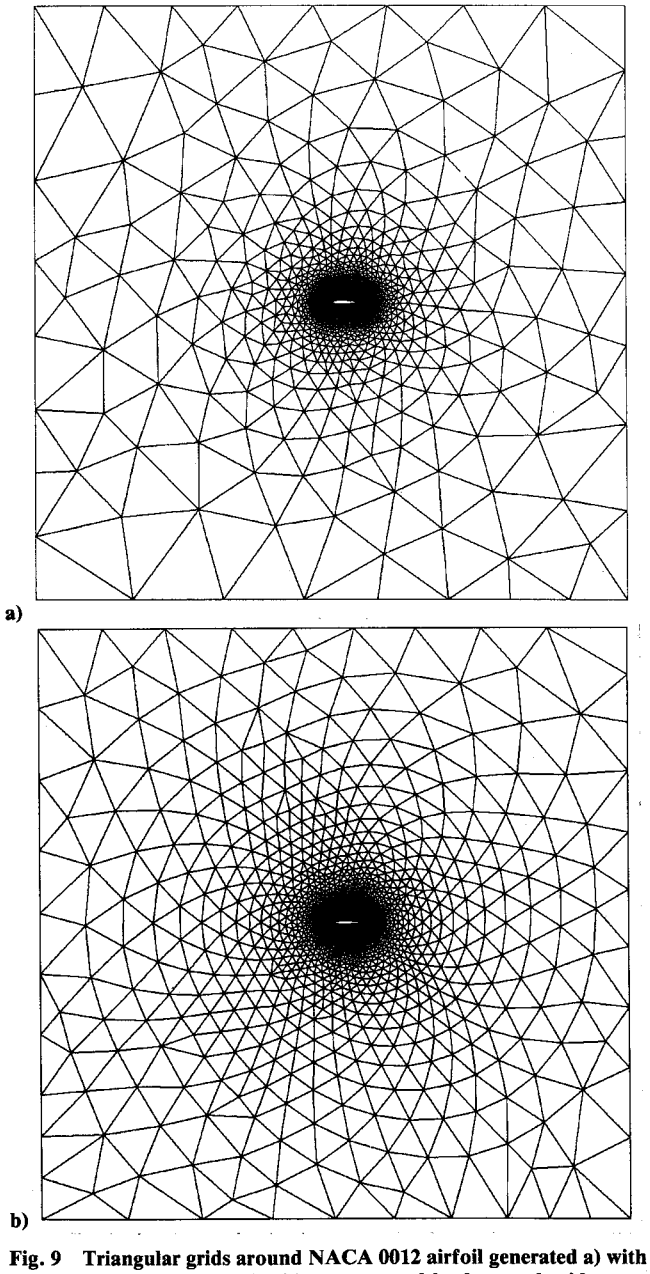

Fig. 9 Triangular grids around NACA 0012 airfoil generated a) with no background grid and b) with a structured background grid.

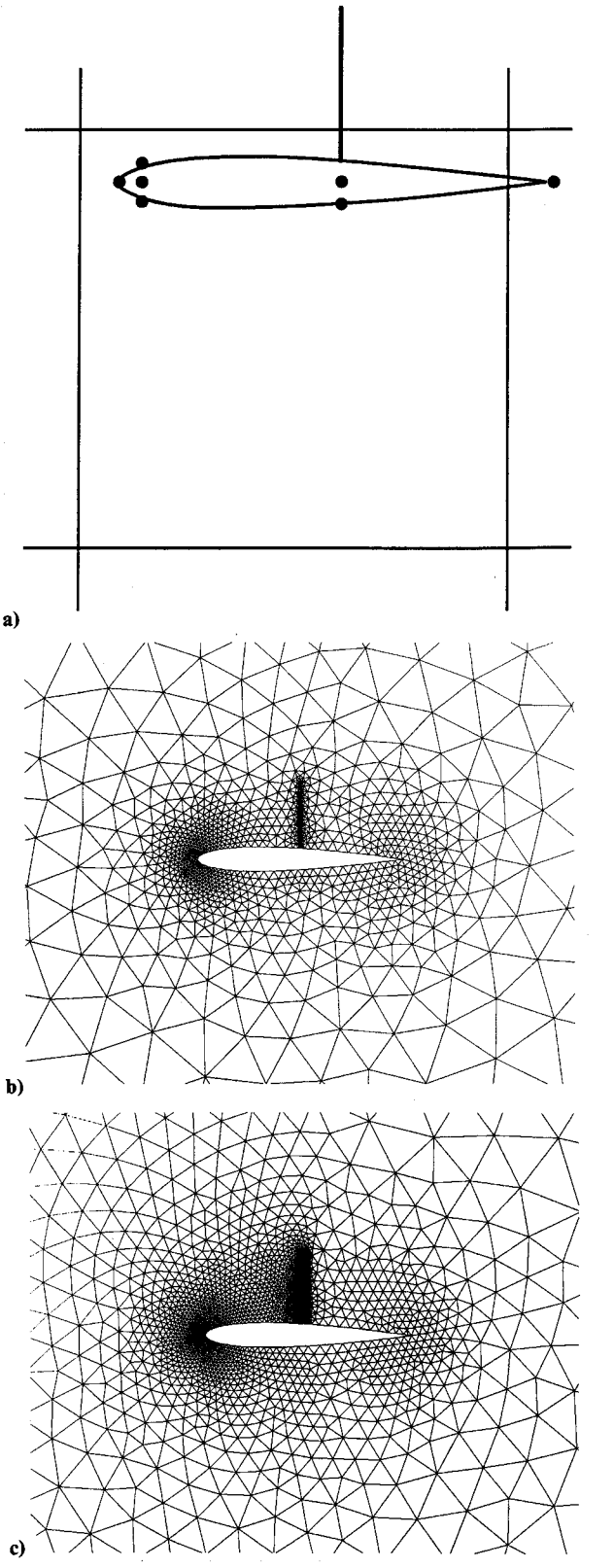

Fig. 10 Local grid refinement by addition of a linear source element: a) background grid, b) and c) triangular grids.

To illustrate the improved grid quality obtained by the new method, two meshes were generated around a NACA 0012

airfoil configuration with a chord length of 1 and a square outer boundary having a side length of 20 units. The first grid was generated with the conventional approach and the other one with the new method. The triangular background grid used for the conventional mesh is shown in Fig. 1 having 22 cells and 16 nodes. A corresponding 21×21 Cartesian background grid is shown in Fig. 2 with an equal number of source elements to the nodes of the unstructured background grid and with the same locations and prescribed spacings. A converged solution for the spacing parameter distribution in the field was obtained in 33 iterations with residuals decreasing by four orders of magnitude. The interpolation of grid spacings for the advancing-front process has been from both the background grid nodes and all of the source elements for this case.

The grid generated using the unstructured background mesh is shown in Fig. 7 and consists of 3047 cells, 1580 points, and 113 boundary nodes. The grid constructed with the new method is shown in Fig. 8 and contains 3063 cells, 1586 points, and 109 boundary nodes. A comparison of these meshes clearly indicates the improvement obtained by the new method. The conventionally generated grid lacks the desired smoothness in distribution, whereas the one generated with the present method exhibits an orderly progression of contours resembling concentric "isotherms" around the configuration. The distribution of points in Fig. 7 appears linear with spacings growing too fast off the surface of the airfoil, whereas in the new grid more points are clustered around the airfoil by simple adjustment of the source intensities.

The effect of the background grid ellipticity is further examined in Fig. 9. Two grids are compared: one generated without a background grid for which the spacings have been interpolated directly from source elements (Fig. 9a) and another gen-

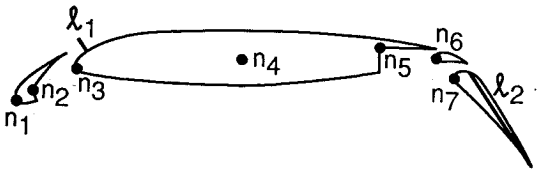

Fig. 11 Multielement airfoil configuration with prescribed nodal and linear source elements.

Table 2 Source parameters for the multielement airfoil grid

Source	a_n	b_n	α	u	S_n
n_1	0.75	0.00	0.0	—	0.0025
n_2	0.45	0.00	0.0	—	0.0035
n_3	0.75	0.00	0.0	—	0.0025
n_4	0.40	0.00	0.0	—	0.0150
n_5	0.70	0.00	1.0	(0.100, −0.995)	0.0030
n_6	0.20	0.60	1.0	(1.000, 0.000)	0.0020
n_7	0.20	0.60	1.0	(1.000, 0.000)	0.0020
ℓ_1	0.10	0.00	0.0	—	0.001, 0.001
ℓ_2	0.35	0.80	1.0	(0.707, 0.707)	0.003, 0.005
n_{b1}	1.30	0.00	0.0	—	3.0000
n_{b2}	1.30	0.00	0.0	—	3.0000
n_{b3}	1.30	0.00	0.0	—	3.0000
n_{b4}	1.30	0.00	0.0	—	3.0000

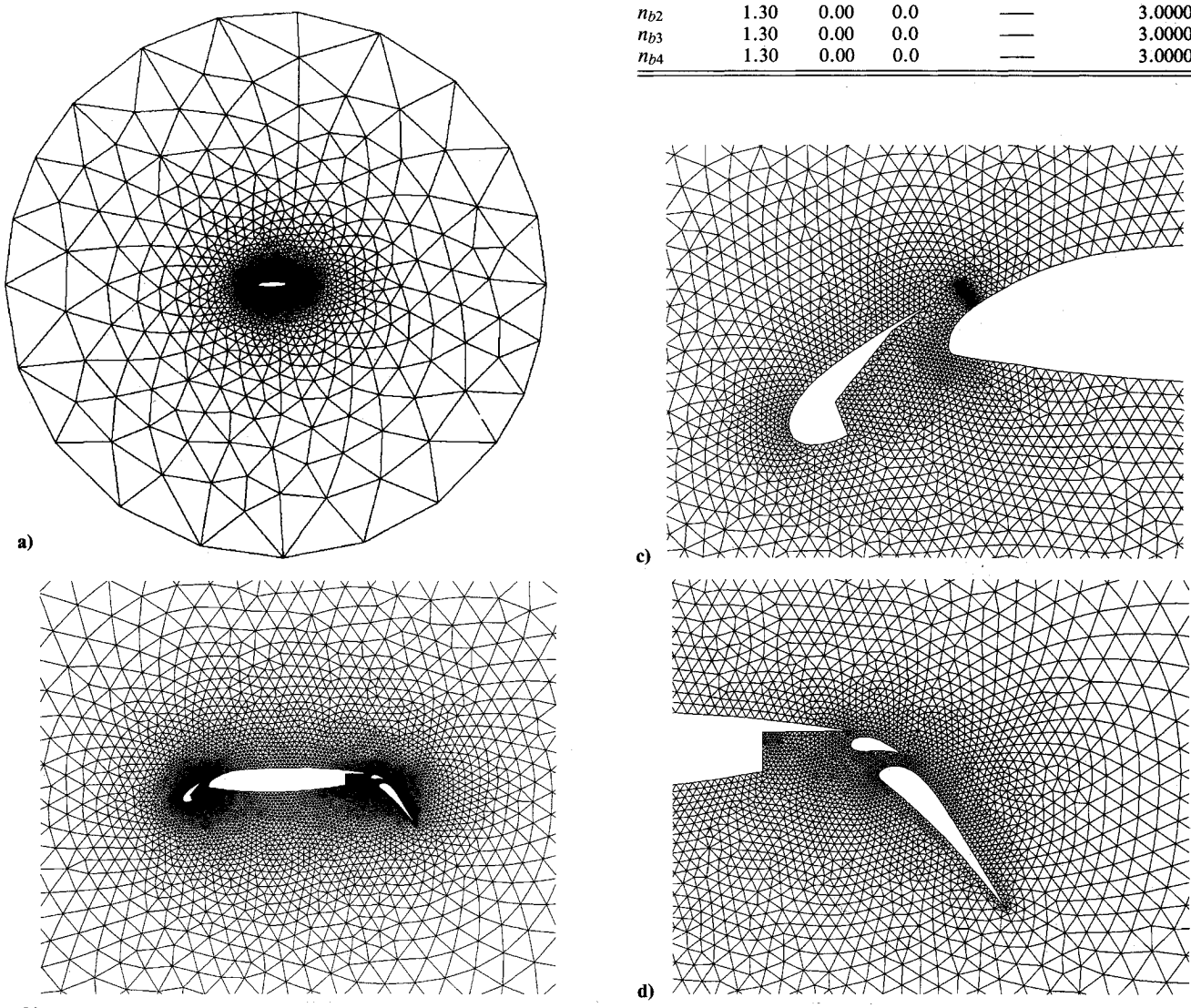

Fig. 12 Triangular grid around a multielement airfoil configuration.

erated by interpolating grid spacings from a 100×100 background grid with a smooth distribution of spacing parameters at the nodes (Fig. 9b). Although the grid in Fig. 9a is acceptable, it is not as smooth as its counterpart and grows rapidly off the inner boundary. The choice of a relatively fine background grid for this case has made up for the omission of source elements from the interpolation process and has produced a good variation of grid spacings throughout the domain. This speeds up the grid-generation process (simple interpolation only from four nodes of a background grid cell); however, the process needs more memory to store a large background grid, particularly for three-dimensional problems, and may still lack the desired grid distribution flexibility.

To demonstrate the versatility of the method and its potential application to solution adaptive gridding, one of the source nodes was replaced with a linear source element on the upper surface of the airfoil to mimic a grid adapted to a shock wave (Fig. 10a). The rest of the original background grid remains unchanged. The results are shown in Figs. 10b and 10c with grid points concentrated at the presumed shock location. The extent of the refined region is easily controlled by adjusting the intensity of the line source as shown. Adaptive unstructured mesh regeneration is typically done by using the current unstructured grid as the background mesh for generating the next grid.[2] This is computationally time consuming and makes the interpolation process complicated, especially for regions of small and skewed cells. In the new method, the original Cartesian background grid would remain intact throughout the process of adaptive grid regeneration; only the source elements should be modified based on the flow characteristics.

The capability of the method has been further examined by generating a grid around a complex multielement airfoil. To complicate the condition even further, the grid has been assumed to be adapted to a hypothetical complex flowfield containing a shock wave. The geometry is composed of four airfoil sections set up in a high-lifting arrangement with a total length of about 1 as shown in Fig. 11. A circular outer boundary for this case has a radius of 6 units. The background grid used is a 81×81 Cartesian mesh with seven nodal and two linear source elements positioned near the airfoil sections (also shown in Fig. 11) and four nodal source elements at the outer boundary to set up the boundary conditions. All nodal elements have symmetrical intensities except the one at the trailing right-angled corner of the main airfoil (n_5) that has a one-sided intensity propagating downward and the two elements at the leading edges of the third and fourth airfoil sections (n_6 and n_7) that propagate streamwise mostly. The linear element on the flap (ℓ_2) has a variable spacing and propagates mainly toward the upper surface of the airfoil. The source parameters used for generating this grid are given in Table 2.

Figure 12 shows the generated grid having 13,636 cells, 7020 points, and 410 boundary nodes. The grid distribution is smooth and efficiently resolves all of the details of the configuration and the flowfield. This example demonstrates the high degree of the mesh flexibility and distribution control that can be achieved with the present method. For example, note the miniature grid refinement at the presumed shock location near the nose of the main airfoil in Fig. 12c as compared with the overall size of the domain in Fig. 12a. The refinement has been made by addition of a small linear source element (ℓ_1) with a weak symmetrical intensity. Also note that the effect of the source element at the trailing corner(n_5) has been confined only to the lower surface in Fig. 12d without influencing the grid resolution on the upper surface of the thin tail section. The observed degree of grid smoothness, variation, and control could not be achieved without interpolating the spacing parameters from both the Cartesian grid nodes and the source elements unless a finer background grid was used. The reproduction of such a detailed grid distribution using the conventional method would require a complex triangular background mesh with many small cells concentrated at the locations of interest.

Concluding Remarks

A new method for construction of background grids has been proposed to improve the generation of unstructured grids using the advancing-front method. The method is based on Cartesian meshes and solution to an elliptic partial differential equation. Because of the simplicity and flexibility of the approach, many of the problems associated with the conventional unstructured grids are resolved.

The construction of background grids by the new method is, for the most part, automatic and requires minimal user interaction. The input data are limited to information about a few source elements such as locations, spacing parameters, and propagation directions of the sources. No grid coordinates and connectivities need to be generated and stored as for unstructured background grids. Unlike the conventional method, the new technique distributes spacing parameters among the nodes of a background grid in a systematic manner. The smoothness of a resulting unstructured grid is guaranteed by solution of the governing elliptic equation.

The new background grids are more flexible to modifications due to the arbitrariness of the location and directional control capability of the source elements. As there is no limit to the number and location of these sources being introduced to the field, a background grid can be modified at any time by simply adjusting the number, type, and/or characteristics of the elements to match the grid requirements. This is specifically useful for adaptive grid refinement/derefinement in which more source elements can be automatically added to the regions of high gradient and removed from locations of uniform flow as dictated by the flow solution.

Finally, interpolation from a uniform Cartesian background grid is convenient since no grid connectivity or additional information about neighboring cells are required. Also there are no search and check operations involved for locating interpolation points in a background grid.

The capability of the new method has been demonstrated for generation of two-dimensional triangular grids. The method is also extendable to three-dimensional problems with minor adjustments and modifications. The significance of the method would be greater for generation of three-dimensional grids since the complexity of conventional tetrahedral background grids is even more extensive.

Acknowledgments

This work was supported by NASA Langley Research Center, Contract NAS1-18585. The author would like to thank Neal Frink (Transonic Aerodynamics Branch, Applied Aerodynamics Division, NASA Langley Research Center) for many invaluable discussions and suggestions and Dimitri Mavriplis (Institute for Computer Applications in Science and Engineering, NASA Langley Research Center) for providing the multielement airfoil configuration.

References

[1]Löhner, R., and Parikh, P., "Generation of Three-Dimensional Unstructured Grids by the Advancing Front Method," *International Journal for Numerical Methods in Fluids,* Vol. 8, No. 10, 1988, pp. 1135–1149.

[2]Peraire, J., Morgan, K., and Peiro, J., "Unstructured Finite Element Mesh Generation and Adaptive Procedures for CFD," *AGARD Conference Proceedings,* No. 464, AGARD, France, 1990, pp. 18.1–18.12.

[3]Parikh, P., Pirzadeh, S., and Löhner, R., "A Package for 3-D Unstructured Grid Generation, Finite-Element Flow Solution and Flow Field Visualization," NASA CR-182090, Sept. 1990.

[4]Peraire, J., Morgan, K., and Peiro, J., "Unstructured Mesh Generation by the Advancing Front Method," *von Kármán Institute for Fluid Dynamics Lecture Series, Numerical Grid Generation,* von Kármán Inst., Brussels, Belgium, June 11–15, 1990, pp. 37–66.

[5]Peiro, J., "A Finite Element Procedure for the Solution of the Euler Equations on Unstructured Meshes," Ph.D. Dissertation, Univ. College of Swansea, Swansea, Wales, UK, Sept. 1989.

[6]Lapidus, L., and Pinder, G. F., *Numerical Solution of Partial Differential Equations in Science and Engineering,* Wiley, New York, 1982, pp. 405–417.